# A BAYESIAN SPARSE INFERENCE APPROACH IN NEAR-FIELD WIDEBAND AEROACOUSTIC IMAGING

*Ning CHU, Ali MOHAMMAD-DJAFARI*

CNRS-SUPELEC-UNIV PARIS SUD
Laboratoire des signaux et systèmes (L2S)
91192 GIF-SUR-YVETTE, FRANCE

*José PICHERAL*

SUPELEC
Dept. Signal et Systèmes Electroniques
91192 GIF-SUR-YVETTE, FRANCE

**ABSTRACT**

Recently improved deconvolution methods using sparse regularization achieve high spatial resolution in aeroacoustic imaging in the low Signal-to-Noise Ratio (SNR), but sparse prior and model parameters should be optimized to obtain super resolution and be robust to sparsity constraint. In this paper, we propose a Bayesian Sparse Inference Approach in Aeroacoustic Imaging (BSIAAI) to reconstruct both source powers and positions in poor SNR cases, and simultaneously estimate background noise and model parameters. Double Exponential prior model is selected for source spatial distribution and hyper-parameters are estimated by Joint Maximized A Posterior criterion and Bayesian Expectation and Minimization algorithm. On simulated and wind tunnel data, proposed approach is well applied for near-field wideband monopole and extended source imaging. Comparing to several classical methods, proposed approach is robust to noise, super resolution, wide dynamic range, and source number and SNR are not needed.

***Index Terms—*** Bayesian sparse inference, near-field wideband, aeroacoustic imaging

## 1. INTRODUCTION

Aeroacoustic imaging is a standard technique for mapping locations and strengths of aeroacoustic sources with microphone arrays. It is widely used for designing quieter vehicles and machinery. In this paper, we aim to investigate a robust approach in near-field wideband aeroacoustic imaging on vehicle surface in wind tunnel test based on the 2D Non-Uniform microphone Array (NUA). Though the Near-field Acoustic Hologram (NAH) provides good resolution over entire frequency band, but it is limited by hologram size and can not work well using sparse array. The beamforming method is simple and fast, but its spatial resolution is limited due to high sidelobes. The MUSIC greatly improves resolutions, but it requires high $SNR$ and source number. The CLEAN iteratively extracts peak sources from a beamforming image, but could not separate sources from severe noises. The Deconvolution Approach for Mapping of Acoustic Source (DAMAS) method [1] becomes a breakthrough and is applied in wind tunnel test by the NASA, however, the DAMAS is sensitive to noise and suffers from slow convergence. The DAMAS2 and DAMAS3 are accelerated by using invariant Point Spread Function (PSF) which inevitably harms resolutions for neal-field application. The Covariance Matrix Fitting (CMF) method [2] is robust to noise, but it is not feasible for high resolution imaging due to its huge variable dimensionality. Recently the Robust DAMAS with Sparse Constraint (SC-RDAMAS) [3] achieves super resolution and estimates noise variance, but the sparsity constraint on total source power is hard to determine in poor SNR. Most of classical methods suffers at least one of these drawbacks: poor spatial resolutions, sensitive to background noise, need for source number and high computational cost.

To overcome most of above drawbacks, proposed approach is to exploit the sparsity of source spatial distributions by applying Bayesian inference. Our novelties are that we apply Double Exponential model as spatial sparse prior to obtain super resolutions in poor SNR, and hyper-parameters are selected by Joint MAP criterion based on Bayesian EM algorithm. The advantages of proposed approach are: source number and SNR are not needed, and it is robust to background noise, super-resolved imaging, wide dynamic range of power estimations and applicable to use in wind tunnel experiments with 2D NUA array.

This paper is organized as follows: In Section 2, formulation of aeroacoustic imaging and classical inverse methods are briefly introduced. Then our approach is proposed in Section 3. Performance comparisons on simulated and real data are correspondingly illustrated in Section 4 and Section 5. Finally we conclude the paper in Section 6.

## 2. FORMULATION OF AEROACOUSTIC IMAGING

### 2.1. Assumptions

Four necessary assumptions are made: Sources are punctual, temporally uncorrelated; noise is Additive Gaussian White Noise (AGWN), independent and identically distributed (iid);

sensors are omnidirectional with unitary gain; and reverberations could be negligible in the anechoic wind tunnel.

### 2.2. Forward propagation model

Consider $M$ antenna sensors and $N$ near-field wideband sources $\boldsymbol{s}(f) = [s_1(f), \cdots, s_N(f)]^T$ at positions $\boldsymbol{p} = [\boldsymbol{p}_1, \cdots, \boldsymbol{p}_N]^T$ with $\boldsymbol{p}_n$ being 3D coordinate of source $n$. The total snapshots $T_0$ measured by each sensor is divided into $I$ segments, where each segment consists of $L$ snapshots. Each segment is then converted into $L$ narrow frequency bins by Fourier Transform. Thus for the segment $i \in [1, T]$ and single frequency $f_l$, $l \in [1, L]$, the observed vector $\boldsymbol{z}_i(f_l) = [z_{i1}(f_l), \cdots, z_{iM}(f_l)]^T$ at antenna array is modeled:

$$\boldsymbol{z}_i(f_l) = \boldsymbol{A}(\boldsymbol{p}, f_l)\boldsymbol{s}_i(f_l) + \boldsymbol{e}_i(f_l) \tag{1}$$

where $\boldsymbol{e}_i(f_l)$ is AGWN noise vector at antenna array, and $\boldsymbol{A}(\boldsymbol{p}, f_l) = [\boldsymbol{a}(\boldsymbol{p}_1, f_l), \cdots, \boldsymbol{a}(\boldsymbol{p}_N, f_l)]$ is $M \times N$ near-field steering matrix, with steering vector:

$$\boldsymbol{a}(\boldsymbol{p}_n, f_l) = [\frac{1}{r_{n,1}} e^{-j2\pi f_l \tau_{n,1}}, \cdots, \frac{1}{r_{n,M}} e^{-j2\pi f_l \tau_{n,M}}]^T \tag{2}$$

where $\tau_{m,n}$ is the propagation time from the source $n$ to antenna $m$, and $r_{n,m}$ is the propagation distance during $\tau_{m,n}$.

### 2.3. Classical inverse solutions

#### 2.3.1. Near-field beamforming

For the given location $\boldsymbol{p}_n$ and single frequency $f_l$, the steering vector $\boldsymbol{a}(\boldsymbol{p}_n, f_l)$ is short as $\boldsymbol{a}_n$. An estimate of the source power $y_n$ locating at the scanning point $n$ can be obtained by the beamforming:

$$y_n = \frac{\tilde{\boldsymbol{a}}_n^H \hat{\boldsymbol{R}} \tilde{\boldsymbol{a}}_n}{\|\tilde{\boldsymbol{a}}_n\|^2} \tag{3}$$

where operator $(\cdot)^H$ denotes the conjugate transpose; $\|\cdot\|$ is vector norm; and the beamforming coefficient $\tilde{\boldsymbol{a}}_n$ is:

$$\tilde{\boldsymbol{a}}_n = [r_{n,1} e^{-j2\pi f_l \tau_{n,1}}, \cdots, r_{n,M} e^{-j2\pi f_l \tau_{n,M}}]^T \tag{4}$$

and the estimation of observed covariance matrix $\boldsymbol{R}$ is $\hat{\boldsymbol{R}} = \frac{1}{I}\sum_{i=1}^{I} \boldsymbol{z}_i(f_l)\boldsymbol{z}_i(f_l)^H$; and $\boldsymbol{R}$ is modeled as

$$\boldsymbol{R} = E\{\boldsymbol{z}_i(f_l)\boldsymbol{z}_i(f_l)^H\} = \boldsymbol{A}\boldsymbol{X}\boldsymbol{A}^H + \sigma^2 \boldsymbol{I} \tag{5}$$

where $\sigma^2$ is noise variance; $\boldsymbol{I}$ is the identical matrix; operator $E\{\cdot\}$ denotes mathematical expectation; and $\boldsymbol{X} = E\{\boldsymbol{s}\boldsymbol{s}^H\}$ is source correlation matrix, with $\boldsymbol{x} = diag(\boldsymbol{X})$ standing for uncorrelated source power vector.

#### 2.3.2. DAMAS [1] method

When total snapshot segment is large enough $I >> 1$, we get $\hat{\boldsymbol{R}} \approx \boldsymbol{R}$. By neglecting noise in equation (5), the DAMAS [1] method is deduced as: $\boldsymbol{y} = \boldsymbol{C}\boldsymbol{x}$, where $\boldsymbol{x} = [x_1, \cdots, x_N]^T$; $\boldsymbol{y} = [y_1, \cdots, y_N]^T$, and power transferring matrix $\boldsymbol{C}$ has the coefficient (PSF) $c_{n,q} = \frac{\|\tilde{\boldsymbol{a}}_n^H \boldsymbol{a}_q\|^2}{\|\tilde{\boldsymbol{a}}_n\|^2}$ with $n, q = 1, \cdots, N$, and $c_{nn} = 1$ for any $q = n$. Its iterative non-negative solution is:

$$\hat{x}_n = y_n - \left[\sum_{q=1}^{n-1} c_{nq}\hat{x}_q + \sum_{q=n+1}^{N} c_{nq}\hat{x}_q\right], \quad \hat{x}_n \geq 0 \tag{6}$$

The DAMAS is a powerful technique to deconvolve the beamforming result. However, its biggest drawback is not robust to noise pollution. Diagonal Removal DAMAS [1] constrains $diag\{\hat{R}\} = 0$ to suppress the noise interference, but it inevitably harms weak sources.

## 3. PROPOSED APPROACH

### 3.1. Bayesian sparse inference

Bayesian inference approach is based on the posterior law:

$$p(\boldsymbol{x}, \boldsymbol{\theta}|\boldsymbol{g}, \boldsymbol{\theta}_0) \propto p(\boldsymbol{g}|\boldsymbol{x}, \boldsymbol{\theta}_1)p(\boldsymbol{x}|\boldsymbol{\theta}_2)p(\boldsymbol{\theta}|\boldsymbol{\theta}_0) \tag{7}$$

where $\boldsymbol{\theta} = [\boldsymbol{\theta}_1, \boldsymbol{\theta}_2]$ represent the hyper-parameters to be estimated, with $\boldsymbol{\theta}_1$ being the direct model parameters and $\boldsymbol{\theta}_2$ being the prior model parameters; and $\boldsymbol{\theta}_0$ are known parameters. The Joint MAP criterion is:

$$(\hat{\boldsymbol{x}}, \hat{\boldsymbol{\theta}}) = argmax_{(\boldsymbol{x}, \boldsymbol{\theta})}\{p(\boldsymbol{x}, \boldsymbol{\theta}|\boldsymbol{g}, \boldsymbol{\theta}_0)\} \tag{8}$$

For sparse prior $p(\boldsymbol{x}|\boldsymbol{\theta}_2)$, aeroacoustic sources sparsely lay out on object surface, and source number is rather fewer than scanning points. Many literatures have explored spatial sparse prior like [4]. For monopole sources, we select a distribution with a sharp summit and short tail among Generalized Gaussian family $\mathcal{GG}(x)$. For uncorrelated centralized variable $x$, the prior model based on $\mathcal{GG}(x)$ is:

$$p(\boldsymbol{x}) = \prod_{n=1}^{N} \mathcal{GG}(x_n|\gamma, \beta) = (\frac{\beta\gamma}{2\Gamma(1/\beta)})^N \exp\left[-\gamma \sum_{n=1}^{N} |x_n|^\beta\right] \tag{9}$$

where probability density function (PDF) of $\mathcal{GG}(x_n|\gamma, \beta)$ is

$$\mathcal{GG}(x_n|\gamma, \beta) = \frac{\beta\gamma}{2\Gamma(1/\beta)} \exp\left[-\gamma |x_n|^\beta\right] \tag{10}$$

where $\Gamma(\cdot)$ is the Gamma function, and $\gamma$ and $\beta$ control PDF pattern. For $0 < \beta < 1$, it is of great interest to enforce sparsity, but its $-ln[\mathcal{GG}(\boldsymbol{x})]$ is not convex. For $\beta = 1$, the Double Exponential (DE) model is spatially sparse, and its $-ln[\mathcal{GG}(\boldsymbol{x})]$ is convex. For source powers $\boldsymbol{x}$, non-negative condition is combined with DE model.

To obtain the likelihood $p(\boldsymbol{y}|\boldsymbol{x}, \sigma^2)$, we propose to use the system error $\boldsymbol{\xi} = [\xi_1, \cdots, \xi_N]$, which represent unpredictable parts in forward propagation model of equation (1):

$$\boldsymbol{\xi} = \boldsymbol{y} - \boldsymbol{C}\boldsymbol{x} - \sigma^2 \boldsymbol{1}_N \tag{11}$$

Assuming $\boldsymbol{\xi} \sim \mathcal{N}(0, \sigma_\xi^2)$, the likelihood $p(\boldsymbol{y}|\boldsymbol{x}, \sigma^2)$ is:

$$p(\boldsymbol{y}|\boldsymbol{x}, \sigma^2) = \frac{1}{(2\pi\sigma_\xi^2)^{N/2}} \exp\left[-\frac{\|\boldsymbol{y} - \boldsymbol{C}\boldsymbol{x} - \sigma^2 \mathbf{1}_N\|^2}{2\sigma_\xi^2}\right] \tag{12}$$

We take Jeffreys prior for positive unknown parameters as $p(\sigma^2) \sim \frac{1}{\sigma^2}$, $p(\sigma_{\boldsymbol{\xi}}^2) \sim \frac{1}{\sigma_{\boldsymbol{\xi}}^2}$ and $p(\gamma) \sim \frac{1}{\gamma}$. Taking equation (12), DE model and Jeffreys prior into equation (8), and omitting small terms as:

$$\mathcal{J}(\boldsymbol{x}, \boldsymbol{\theta}) = \frac{\|\boldsymbol{y} - \boldsymbol{C}\boldsymbol{x} - \sigma^2 \mathbf{1}_N\|^2}{2\sigma_{\boldsymbol{\xi}}^2} + \gamma\|\boldsymbol{x}\|_1 + \frac{N}{2} ln\sigma_{\boldsymbol{\xi}}^2 + N ln\gamma \tag{13}$$

where $\boldsymbol{\theta} = [\sigma^2, \sigma_{\boldsymbol{\xi}}^2, \gamma]$. The hyper-parameters is optimized by Bayesian EM algorithm based on simple initialization of $\boldsymbol{x}$:

$$\begin{cases} E - step: & q(\boldsymbol{\theta}, \hat{\boldsymbol{\theta}}^{(k-1)}) = E_{p(\boldsymbol{x}|\boldsymbol{g}, \hat{\boldsymbol{\theta}}^{(k-1)})}[\mathcal{J}(\boldsymbol{x}, \boldsymbol{\theta})] \\ M - step: & \hat{\boldsymbol{\theta}}^{(k)} = argmax_{(\boldsymbol{\theta})}\{q(\boldsymbol{\theta}, \hat{\boldsymbol{\theta}}^{(k-1)})\} \end{cases} \tag{14}$$

We alternatively optimize $\boldsymbol{x}$ based on $\hat{\boldsymbol{\theta}}$ by the MAP and repeat EM procedure for better $\hat{\boldsymbol{\theta}}$ based on $\hat{\boldsymbol{x}}$ until convergence.

### 3.2. Wideband estimation

In wind tunnel experiment, aeroacoustic sources are generated by the friction and collision between the vehicle and wind flow. Physically, different vehicle parts with various sizes produce vibrations with different frequencies. Therefore aeroacoustic sources are near-field wideband signals. Consider the frequency range $[f_{min}, f_{max}]$ consisting of $L$ frequency bins. Let $\hat{\boldsymbol{x}}(f_l)$ be the estimation of $\boldsymbol{x}(f_l)$ in $l$th frequency bin. Then source powers $\boldsymbol{x}_{wb}$ over wideband $[f_{min}, f_{max}]$ can be estimated by $\hat{\boldsymbol{x}}_{wb} = \frac{1}{L}\sum_{f_l=f_{min}}^{f_{max}} \hat{\boldsymbol{x}}(f_l)$.

## 4. SIMULATION

The simulations and experiments use the same configurations. There are 64 2D NUA array on vertical plane, whose averaging array aperture is $d = 2m$ with longer horizontal aperture, as shown in Fig.2a. For NUA array, it yields almost the same performance as the uniform array with more sensors does. The distance between source plane and array is around $R = 4.50m$, thus the beamforming resolution at $f = 2500Hz$ is $\Delta B \approx \lambda R/d = 31cm$. For scanning step, we choose $\Delta x = 5cm$ to satisfy $\Delta x/\Delta B < 0.2$ for any $f < 3500Hz$, which avoids the spatial aliasing in the DAMAS [1]. The propagation speed is $c_0 \approx 340m/s$. There are $T_0 = 10000$ snapshots and averaging $SNR = 0dB$. Results are illustrated by decibel (dB) images and section profiles.

In Fig.1a, there are 4 monopoles and 5 extended sources with different patterns; their powers are $0.08 \sim 2$ ($-10.27 \sim 3.7dB$) with $14dB$ dynamic range. The noise is $\sigma^2 = 0.85$ ($-0.7dB$). As shown in Fig.1 and averaging estimation error $\overline{\Delta x}$ in Table 1, the beamforming hardly separates any sources; both the DR-DAMAS and CMF fails to detect weak sources; the SC-RDAMAS estimates noise variance and works better than the CMF, but proposed method outperforms the above methods regardless of source patterns and positions on scanning plane.

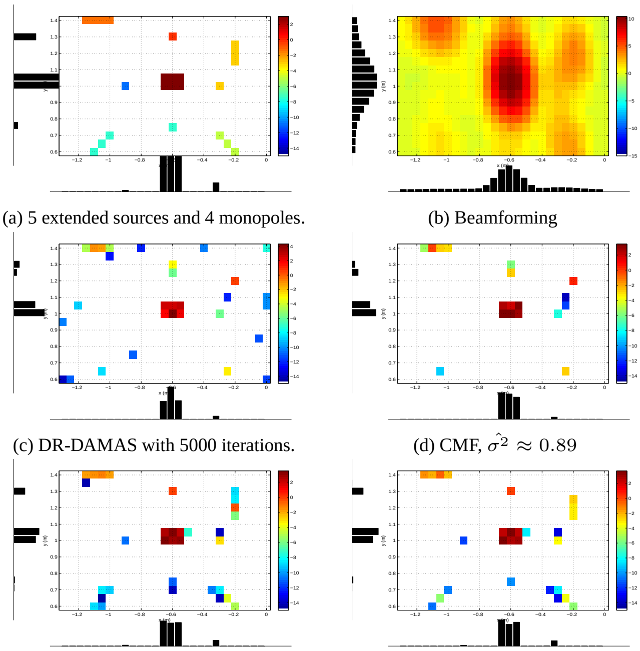

(a) 5 extended sources and 4 monopoles. (b) Beamforming

(c) DR-DAMAS with 5000 iterations. (d) CMF, $\hat{\sigma^2} \approx 0.89$

(e) SC-RDAMAS, $\hat{\sigma^2} \approx 0.86$ (f) Proposed, $\hat{\sigma^2} \approx 0.85$

**Fig. 1.** Simulations at $SNR = 0dB$ and $f = 2500Hz$.

| Source powers | 0.08 | 0.18 | 0.98 | 0.50 | $\overline{\Delta x}$ (%) |
|---|---|---|---|---|---|
| Beamforming | 1.57 | 11.28 | 3.51 | 2.02 | 4.16 |
| DR-DAMAS | - | - | 0.77 | 0.23 | 0.19 |
| CMF | 0.09 | - | 0.80 | 0.40 | 0.12 |
| SC-RDAMAS | 0.09 | 0.10 | 1.05 | 0.43 | 0.06 |
| Proposed | 0.08 | 0.13 | 0.94 | 0.45 | 0.04 |

**Table 1.** Monopole source power estimations.

## 5. HYBRID DATA

Figure 2 shows configurations of wind tunnel S2A [5]. The scanning region is $135 \times 470cm^2$. There are $T_0 = 524288$ snapshots, $I = 204$ segments, $L = 2560$ snapshots per segment. Wideband is $2400Hz - 2600Hz$ with $B = 21$ frequency bins. The results are shown by normalized dB images with $10dB$ span. For corrections of propagation time $\tau_{n,m}$ and distance $r_{n,m}$, we apply equivalent source that antenna $m$ seems to receive the signal from equivalent source $n'$ along a direct line $d_{n',m}$ during the same propagation time $\tau_{n',m}$, as if there is no wind influence, as shown in Fig.2b.

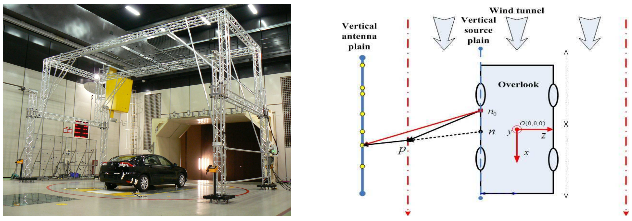


(a) Wind tunnel S2A [5].  (b) Overlook and wind tunnel effect.

**Fig. 2**. Configurations of wind tunnel S2A.

Five synthetic extended sources with different patterns are added to real data of wind tunnel experiment in the Fig.3a, whose powers are from $-4.5$ to $0dB$. Figure 3 shows that for synthetic sources, proposed approach successfully detect most of them with more precise estimations of source positions and powers; meanwhile, for real data, proposed method better reconstruct both strong and weak sources on two wheels, rear-view mirror and windows, and better suppresses background noise, comparing to the state of art methods: the beamforming, DR-DAMAS and SC-RDAMAS.

### 6. CONCLUSIONS

We propose a Bayesian Sparse Inference Approach in Aeroacoustic Imaging (BSIAAI) to reconstruct both source positions and powers in poor SNR case, and simultaneously estimate background noise and model parameters. Hyperparameters are estimated by Joint MAP criterion based on Bayesian EM algorithm. Advantages of our method are: source number and SNR are not needed; and it is robust to noise, wide dynamic range of power estimation, super resolutions and feasible to use in the wind tunnel tests based on 2D NUA array. Its effectiveness is compared with the state-of-art methods for near-field wideband uncorrelated monopole and extended source imaging on simulated and experiment data. For further works, we are considering colorful noise interference and multi-path reflection effect.

## Acknowledgment

Authors gratefully thank Renault SAS for offering real data.

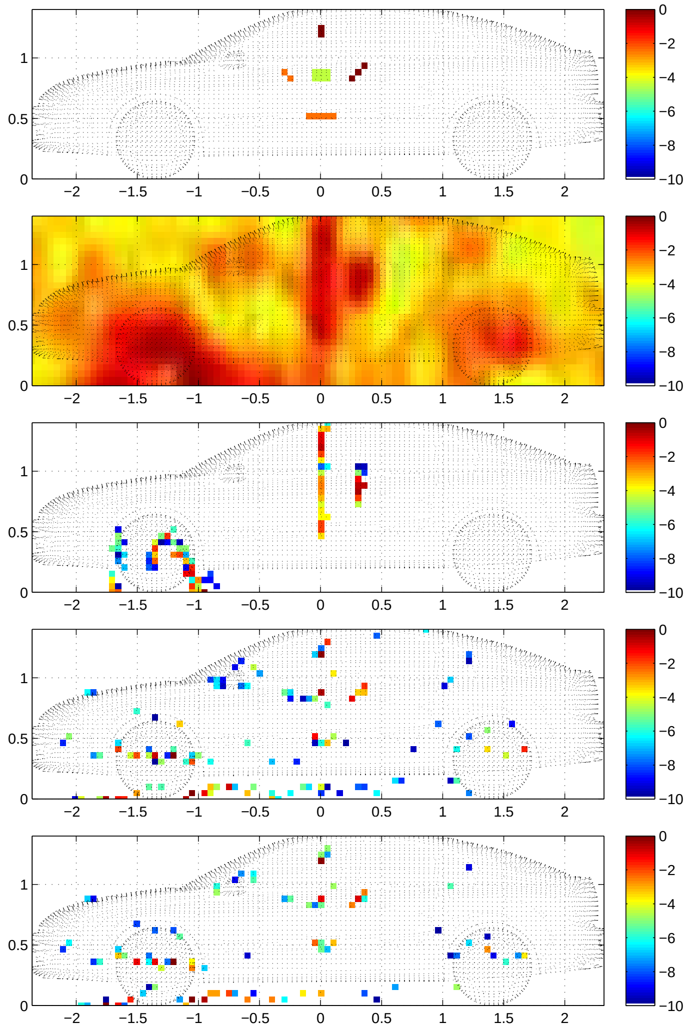

**Fig. 3**. Acoustic imaging for hybrid data at $[2400-2600]Hz$. From top to bottom: Synthetic sources, Beamforming, DR-DAMAS, SC-RDAMAS, Proposed

### 7. REFERENCES

[1] T.F. Brooks and W.M. Humphreys, "A deconvolution approach for the mapping of acoustic sources (DAMAS) determined from phased microphone arrays," *Journal of Sound and Vibration*, vol. 294, no. 4-5, pp. 856–879, 2006.

[2] Tarik Yardibi, Jian Li, Petre Stoica, Nikolas S. Zawodny, and Louis N. Cattafesta, "A covariance fitting approach for correlated acoustic source mapping," *Journal of The Acoustical Society of America*, vol. 127, 2010.

[3] N. CHU, J. Picheral, and A. M. Djafari, "A robust super-resolution approach with sparsity constraint for near-field wideband acoustic imaging," in *IEEE International Symposium on Signal Processing and Information Technology*, Bilbao, Spain, Dec 14-17,2011, pp. 286–289.

[4] Ali Mohammad-Djafari, "Bayesian approach with prior models which enforce sparsity in signal and image processing," *EURASIP Journal on Advances in Signal Processing*, vol. Special issue on Sparse Signal Processing, 2012.

[5] Arnaud Menoret, Nathalie Gorilliot, and Jean-Luc Adam, "Imagerie acoustique en soufflerie S2A," in *10ème Congrès Français d'Acoustique*, Société Française d'Acoustique SFA, Ed., Lyon, France, 2010.